Ablation of 4E-BP1/2 Prevents Hyperglycemia-Mediated Induction of VEGF Expression in the Rodent Retina and in Müller Cells in Culture

Tabitha L. Schrufer,[1] David A. Antonetti,[1] Nahum Sonenberg,[2] Scot R. Kimball,[1] Thomas W. Gardner,[1,3] and Leonard S. Jefferson[1]

OBJECTIVE—Vascular endothelial growth factor (VEGF) contributes to diabetic retinopathy, but control of its expression is not well understood. Here, we tested the hypothesis that hyperglycemia mediates induction of VEGF expression in a eukaryotic initiation factor 4E (eIF4E) binding protein (4E-BP) 1 and 2 dependent manner.

RESEARCH DESIGN AND METHODS—The retina was harvested from control and type 1 diabetic rats and mice and analyzed for VEGF mRNA and protein expression as well as biomarkers of translational control mechanisms. Similar analyses were performed in Müller cell cultures exposed to hyperglycemic conditions. The effect of 4E-BP1 and 4E-BP2 gene deletion on VEGF expression was examined in mice and in mouse embryo fibroblasts (MEFs).

RESULTS—Whereas VEGF mRNA in the retina remained constant, VEGF expression was increased as early as 2 weeks after the onset of diabetes. Increases in expression of 4E-BP1 protein mirrored those of VEGF and expression of 4E-BP1 mRNA was unchanged. Similar results were observed after 10 h of exposure of cells in culture to hyperglycemic conditions. Importantly, the diabetes-induced increase in VEGF expression was not observed in mice deficient in 4E-BP1 and 4E-BP2, nor in MEFs lacking the two proteins.

CONCLUSIONS—Hyperglycemia induces VEGF expression through cap-independent mRNA translation mediated by increased expression of 4E-BP1. Because the VEGF mRNA contains two internal ribosome entry sites, the increased expression is likely a consequence of ribosome loading at these sites. These findings provide new insights into potential targets for treatment of diabetic retinopathy. ***Diabetes*** **59:2107–2116, 2010**

Diabetic retinopathy is the leading cause of acquired blindness among U.S. citizens under the age of 65, affecting 5.3 million people, or 2.5% of the population (1). Diabetic retinopathy includes both a nonproliferative stage, characterized by vascular tortuosities, macular edema, microaneurysms and lipid exudates, and a proliferative stage, characterized by vascular angiogenesis and potentially severe hemorrhages. Examination of vitreous fluid from the eyes of patients with proliferative diabetic retinopathy demonstrates an increase in vascular endothelial growth factor (VEGF) (2–6). Similarly, an increase in VEGF has been observed in the retina of animal models of diabetes and ischemia. Because VEGF can promote both vascular permeability and angiogenesis, studies on the mechanisms of diabetes-induced VEGF expression and the effect of VEGF on retinal vascular function have been areas of intense study. Changes in glycemia, advanced glycation end products, and localized regions of hypoxia have all been proposed as mediating an increase in VEGF expression. Moreover, overexpression of functional VEGF in normal tissue results in vascular changes similar to those seen in diabetic retinopathy (7,8). In contrast, inhibition of VEGF function in the retina by VEGF-neutralizing agents such as anti-VEGF antibodies (9), overexpression of dominant negative or chimeric Flt-1/VEGF receptors (10,11), or inhibition of receptor tyrosine kinases (12) has been shown to attenuate the abnormal vascular changes associated with the disease.

Expression of VEGF is regulated through multiple transcriptional and posttranscriptional mechanisms. Oxygen tension controls VEGF gene expression through the transcription factor, hypoxia-inducible factor-1α (HIF-1α) (13). During periods of low oxygen tension, for example, ischemia, HIF-1α is stabilized by interaction with HIF-1β, preventing its proteasome-mediated degradation, as well as promoting enhanced transcription of specific genes, such as VEGF (11,14). The architecture of the VEGF mRNA 5′-untranslated region (UTR) also contributes to regulation of VEGF expression through translational control mechanisms. The VEGF mRNA 5′-UTR is longer than average and contains stretches of stable G–C pairing and areas of complementarity that act to repress translation of the coding region under normal physiological conditions. Translation of such mRNAs is thought to occur through a mechanism that does not require ribosome loading at the 5′-m^{7}GTP cap structure (15). The VEGF message contains two putative internal ribosome entry sites that allow for cap-independent translation under conditions of global translation repression (16,17).

The selection of mRNAs for translation is regulated in part by the mRNA cap-binding complex, eIF4F, which is composed of eIF4E, eIF4G, and eIF4A. This complex serves as an intermediate between the m^{7}GTP cap and the 40S ribosomal subunit and is required for cap-dependent binding of mRNA to the ribosome. Assembly of the eIF4F complex is regulated by a class of eIF4E-binding proteins (4E-BPs) that inhibit translation by sequestration of eIF4E

From the [1]Department of Cellular and Molecular Physiology, The Pennsylvania State University College of Medicine, Hershey, Pennsylvania; the [2]Department of Biochemistry, McIntyre Medical Science Bldg., Montreal, Quebec, Canada; the [3]Department of Ophthalmology, The Pennsylvania State University College of Medicine, Hershey, Pennsylvania.

Corresponding author: Scot R. Kimball, skimball@psu.edu.

Received 29 January 2010 and accepted 27 May 2010. Published ahead of print at http://diabetes.diabetesjournals.org on 14 June 2010. DOI: 10.2337/db10-0148.

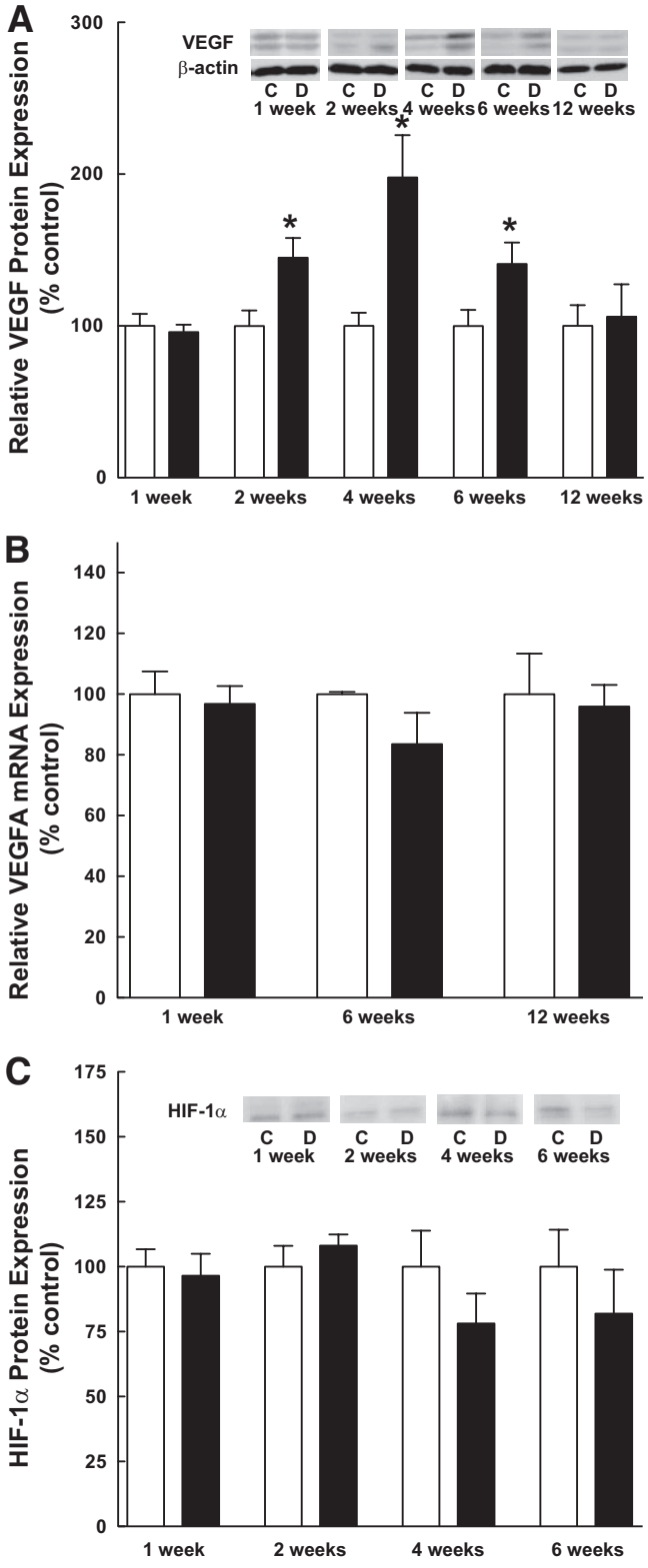

FIG. 1. VEGF expression is increased in the retina of diabetic rats in the absence of changes in VEGF mRNA. *A*: Western blot analysis of VEGF expression. VEGF expression was analyzed in retinal samples from 13 control and 14 diabetic rats at 1 week, 12 control and 14 diabetic rats at 2 weeks, 12 control and 12 diabetic rats at 4 weeks, 13 control and 13 diabetic rats at 6 weeks, and 5 control and 7 diabetic rats at 12 weeks as described in RESEARCH DESIGN AND METHODS. The antibody used in these studies recognizes the 121, 165, and 189 splice variants of VEGF. The molecular weights of the two bands detected by Western blot correspond to the 165 and 189 splice variants. VEGF-A binds to both the VEGF receptor 1 (VEGFR1) and VEGFR2. Activation of the receptors leads to increased vascular permeability and upregulated angiogenesis. Values represent the mean expressed as a percentage of the control value ± SEM; control (white bars) and diabetic (black bars) animals. *B*: Quantitative RT-PCR of VEGF mRNA. Total RNA was extracted from the retina of 6 control and 9 diabetic rats at 4 weeks, 3 control and 6 diabetic rats at 6 weeks, and 10 control and 10 diabetic rats at 12 weeks as described under RESEARCH DESIGN AND METHODS. Values represent the mean expressed as a percentage of an internal β-actin control ± SEM. *C*: Western blot analysis of HIF-1α protein expression. HIF-1α protein expression was analyzed in retinal samples from 5–6 control and 4–5 diabetic rats at each time point as described in RESEARCH DESIGN AND METHODS. Values represent the mean expressed as a percentage of the control value ± SEM. *$P < 0.05$ versus corresponding control value.

away from eIF4G and eIF4A (18). Three 4E-BPs have been identified (4E-BP1, -BP2, and -BP3), and, although each is encoded by a separate gene, their protein sequences are highly conserved, especially in the region containing the eIF4E binding domain. In contrast to 4E-BP1 and -BP2, which are expressed in a variety of tissues, the distribution of 4E-BP3 is restricted. In the hypophosphorylated state, 4E-BPs compete with eIF4G for binding to eIF4E and prevent eIF4F complex assembly (19,20), leading to a decrease in cap-dependent, and a simultaneous increase in cap-independent, mRNA translation. When phosphorylated by the mammalian target of rapamycin complex 1, 4E-BP releases from eIF4E, allowing it to assemble into the eIF4F complex.

In the present study, we show that VEGF expression in the retina is increased at early time points in three different animal models of type 1 diabetes. The increase occurs despite unchanged expression of VEGF mRNA and in the absence of a change in HIF-1α expression, suggesting that it is independent of transcriptional regulation and is likely a result of increased translation of the VEGF mRNA. 4E-BP1 protein content in the retina of diabetic animals is also increased in the absence of a change in its mRNA abundance. Increased 4E-BP1 expression leads to sequestration of eIF4E, resulting in increased VEGF mRNA translation. This conclusion is supported by the observation that the effect is not observed in mice lacking 4E-BP1 and 4E-BP2. These diabetes-induced effects are likely a consequence of hyperglycemia, because in three different cell lines, hyperglycemic conditions promote increased expression of both 4E-BP1 and VEGF, independent of changes in the abundance of their mRNAs. Moreover, similar to what is observed in the retina of diabetic mice, the hyperglycemia-induced increase in VEGF expression in mouse embryo fibroblasts (MEFs) requires 4E-BP1. Overall, the results indicate that diabetes-induced hyperglycemia mediates increased expression of 4E-BP1, leading to enhanced translation of the VEGF mRNA.

RESEARCH DESIGN AND METHODS

Male Sprague-Dawley rats (120–180 g) were housed in The Pennsylvania State University College of Medicine Animal Facility in accordance with Institutional Animal Care and Use Committee (IACUC) guidelines. Type 1 diabetes was induced in rats by a single intraperitoneal injection of streptozotocin (STZ), as previously described (21). Rats exhibiting blood glucose levels above 250 mg/dl, measured 24 h after drug administration, were considered diabetic. Average blood glucose values for the animal models used herein are shown in supplementary Fig. 1 in the online appendix available at http://diabetes.diabetesjournals.org/cgi/content/full/db10-0148/DC1.

Male C57BL/6J Ins2^{Akita} heterozygous mice were bred in The Pennsylvania State University College of Medicine Juvenile Diabetes Research Foundation Diabetic Retinopathy Center Animal Core, in accordance with IACUC guidelines. At 4.5 weeks of age, mice were genotyped and tested for a diabetic phenotype, that is, a blood glucose level exceeding 250 mg/dl. Wild-type littermates were used as controls (22).

Wild-type and *Eif4ebp1*;*Eif4ebp2* double knockout mice were described previously (23). At 4 weeks of age, type 1 diabetes was induced according to the AMDCC "Low-Dose Streptozotocin Induction Protocol (Mouse)" (24). Mice with blood-glucose levels exceeding 250 mg/dl each week were considered diabetic, and those that did not meet this threshold were excluded from the study.

Cell culture. TR-MUL [kindly provided by Dr. Ken-ichi Hosoya (Toyama Medical and Pharmaceutical University)] and Moorfields/Institute of Ophthalmology-Müller 1 [kindly provided by Dr. G. Astrid Limb (University College of London)] retinal Müller cells, and wild-type and *Eif4ebp1*;*Eif4ebp2* double knockout MEFs (23) were maintained in Dulbecco's modified Eagle's medium containing 5.6 mmol/l glucose and 2% heat-inactivated FBS and grown to subconfluence before seeding. Cells were maintained at either 37°C (MIO-M1 and MEFs) or 33°C (TR-MUL), in a humidified, 5% CO_2 atmosphere. TR-MUL and MIO-M1 cells (500,000) were seeded into 6-well dishes, and MEF cells (20,000) were seeded into 12-well dishes and grown to ~75% confluence. Culture medium was aspirated, cells were washed with sterile PBS, and experimental medium was added. For studies of the effects of hyperglycemic conditions, cells were either replenished with medium containing 5.6 mmol/l glucose and 25 mmol/l mannitol (hereafter referred to as control medium) or 25 mmol/l glucose and 10% heat-inactivated FBS (hereafter referred to as high-glucose medium) for 10 h (unless otherwise indicated).

Protein analysis. At the indicated time points, the retina was isolated, flash-frozen in liquid nitrogen, and later sonicated in 500 μl of extraction buffer (25) supplemented with inhibitors [microcystin, sodium vanadate, benzamidine, and protease inhibitor cocktail (Sigma-Aldrich)]. The homogenate was centrifuged at 12,000 rpm for 10 min at 4°C, and the supernatant was collected, a fraction of which was added to 1× Laemmli buffer and boiled for 5 min. For Western blot analysis of these samples, 60 μg of protein was loaded per lane. In studies using cells in culture, medium was collected for VEGF analysis, and cells were washed in sterile PBS, then scraped in 200 μl of either 1× Laemmli buffer, immunoprecipitation homogenization buffer (20 mmol/l HEPES, 2 mmol/l EGTA, 50 mmol/l NaF, 100 mmol/l KCl, 0.2 mmol/l EDTA, 50 mmol/l β-glycerophosphate, pH 7.4, 1 mmol/l benzamidine, 0.5 mmol/l sodium vanadate, 1 μmol/l microcystin, and 15 μl/ml protease inhibitor cocktail), or Lambda phosphatase buffer (26), supplemented with inhibitors (except microcystin and sodium vanadate). For Western blot analysis of these samples, 30 μg of protein was loaded per lane. Protein was separated by SDS-PAGE on 15%, 4–15%, or 4–20% Criterion gels (Bio-Rad Laboratories) and transferred to a polyvinylidene fluoride membrane. The membrane was blocked in 5% milk in Tris-buffered saline Tween-20, washed, and then incubated overnight at 4°C with primary antibody. The source of polyclonal antibodies, and the dilutions used in Western blot analysis, are presented in supplementary Table 1, available in an online appendix. Monoclonal antibodies to the α-subunit of eIF2, eIF4E, and eIF4G were prepared in our laboratory as described previously (27–29). The membranes were incubated with horseradish peroxidase-conjugated secondary antibody, washed, incubated for 1 h at a 1:10,000 dilution, and then developed using enhanced chemiluminescence. Quantitation was performed using a GeneGnome HR imaging system with GeneTools software (SynGene).

For analysis of VEGF production in cells in culture, media was collected from control and treated cells and subjected to VEGF ELISA (Qiagen) following the manufacturer's protocol. VEGF concentration was normalized to total cellular protein content.

Lambda phosphatase treatment. The retinas and harvested cells were sonicated in 500 and 200 μl, respectively, of Lambda phosphatase buffer (26), supplemented with benzamidine and protease inhibitor cocktail, and the homogenate was combined with 4 μl (1,600 units) of Lambda phosphatase and incubated for 1 h at 37°C. The sample was centrifuged at 1,000 g for 3 min, and the supernatant was boiled for 3 min, combined with 2× Laemmli buffer, boiled again for 5 min, and subjected to Western blot analysis.

Analysis of eIF4E:4E-BP interaction. BioMag goat-anti-mouse IgG magnetic beads (BioClone Inc.) (1.5 ml/sample) were washed thrice in low salt buffer (20 mmol/l Tris-HCl, pH 7.4, 5 mmol/l EDTA, 150 mmol/l NaCl, 0.5% Triton X-100, 0.1% β-mercaptoethanol) and then resuspended in 1/5 of the original volume in low salt buffer. Beads were combined with 175 μl PBS, 12.5 μl Triton X-100, and 4 μg monoclonal anti-eIF4E antibody (per sample) and incubated on an orbital rocker overnight at 4°C. On the day of the study, the retinas were homogenized using a Dounce homogenizer in 500 μl of eIF4E homogenization buffer (20 mmol/l HEPES, 2 mmol/l EGTA, 50 mmol/l sodium fluoride, 100 mmol/l potassium chloride, 0.2 mmol/l EDTA, 50 mmol/l β-glycerophosphate, pH 7.4) plus inhibitors. Alternatively, cells in culture were harvested in immunoprecipitation buffer containing 2.5% Triton X-100 and 0.25% deoxycholate. Retinal or cell homogenate was added to 1 ml or 200 μl, respectively, of BioMag bead-bound eIF4E antibody and incubated for 1 h at 4°C. The beads were washed, resuspended in 1× Laemmli buffer, and boiled

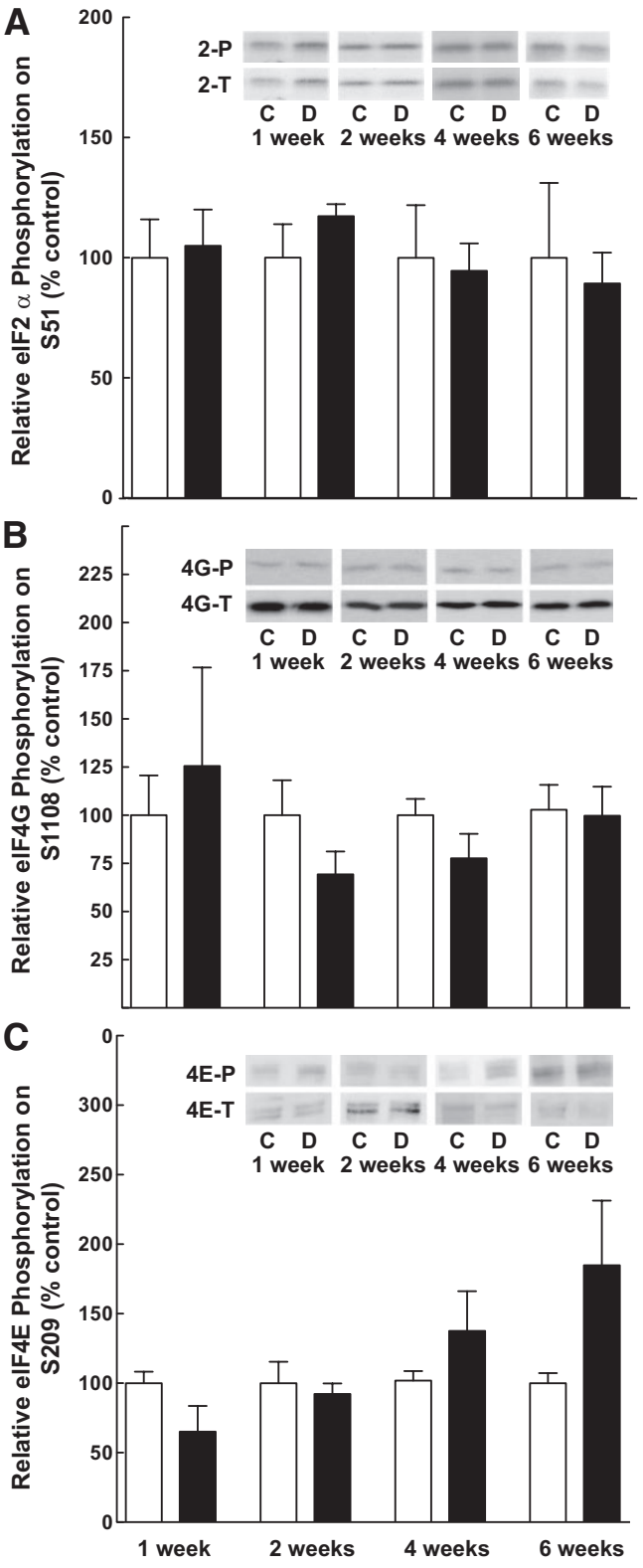

FIG. 2. The relative phosphorylation of a number of biomarkers of mRNA translational control is unchanged in the retina after induction of diabetes. Samples from retinal homogenates prepared as described in RESEARCH DESIGN AND METHODS were assessed for the relative phosphorylation of (*A*) eIF2α on Ser51, (*B*) eIF4G on Ser1108, and (*C*) eIF4E on Ser209. Values for phosphorylation status were normalized to the amount of the respective total protein. Values represent the mean ± SEM of at least three independent sets of animals at each time point (n = 2–4 within each set), except that the control value for eIF2α at 6 weeks represents two animals. Control (white bars) and diabetic (black bars) animals.

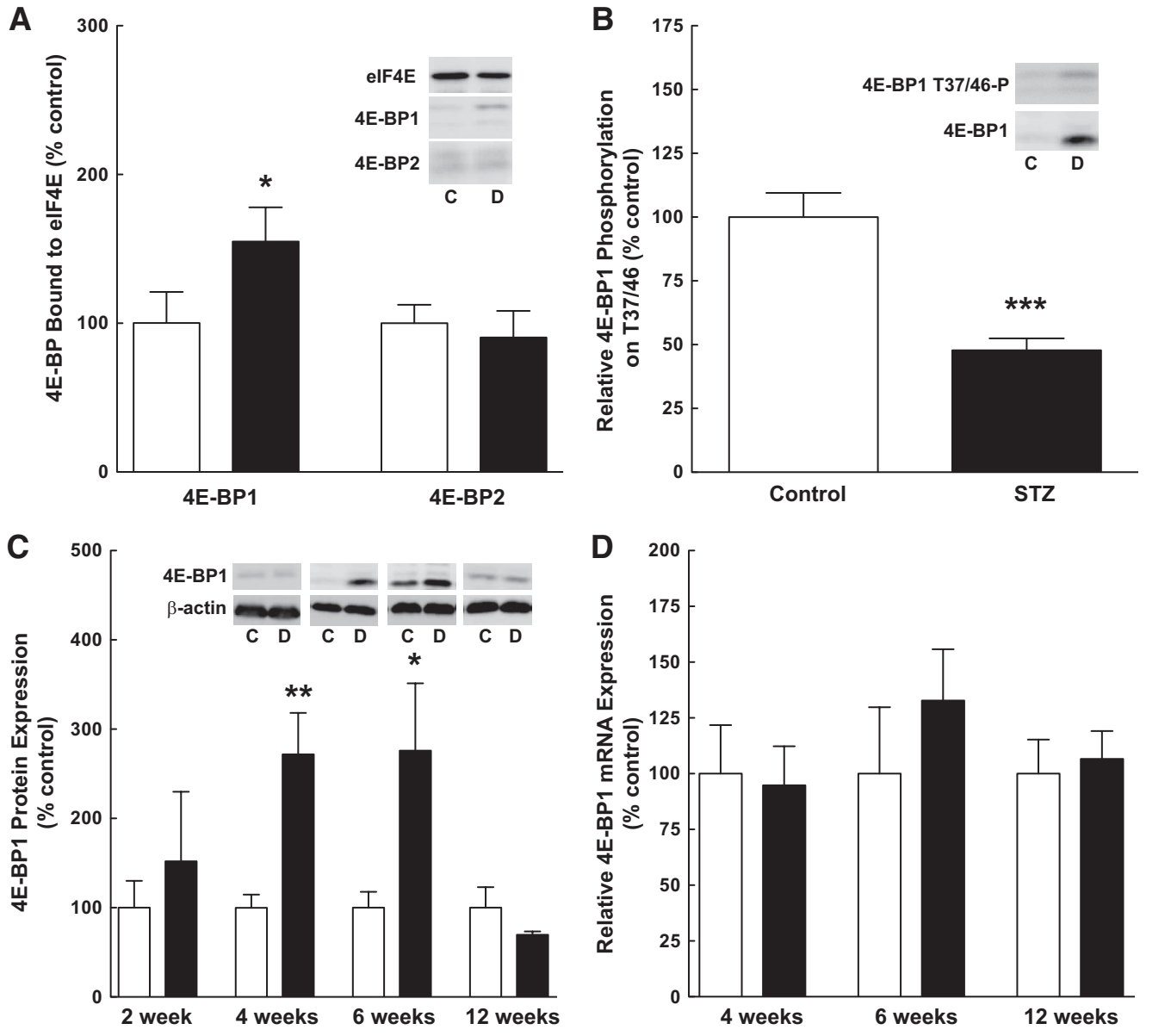

FIG. 3. Enhanced association of 4E-BP1 with eIF4E in the retina of diabetic rats is a result of decreased phosphorylation and increased expression of 4E-BP1. *A*: eIF4E immunoprecipitation. eIF4E immunoprecipitation was carried out as described in RESEARCH DESIGN AND METHODS. Twenty μL of sample was loaded per well. The amount of 4E-BP1 and 4E-BP2 present in the immunoprecipitate was normalized to eIF4E and displayed as a percentage of the control mean ± SEM (n = 8); control (white bars) and diabetic (black bars) animals. *B*: Western blot analysis of 4E-BP1 phosphorylation. 4E-BP1 phosphorylation on T37/46 was normalized to total 4E-BP1 measured from 12 control and 12 diabetic rat retinal extracts 4 weeks after the induction of diabetes; values are displayed as a percentage of the control mean ± SEM. *C*: Western blot analysis of 4E-BP1 expression. Sixty μg of protein was loaded per lane. Representative blots are shown. *D*: Quantitative RT-PCR of 4E-BP1 mRNA. Retinal RNA was extracted as described in RESEARCH DESIGN AND METHODS from 6 control and 9 diabetic rats at 4 weeks, 3 control and 6 diabetic rats at 6 weeks, and 10 control and 10 diabetic rats at 12 weeks. Values represent the mean expressed as a percentage of internal β-actin control ± SEM. *P < 0.05, **P < 0.01, ***P < 0.001 versus corresponding control value.

for 5 min. After the beads were removed, 20 μl of sample was loaded onto a 4–15% Criterion gel and subjected to Western blot analysis.

Quantitative real-time PCR. RNA was isolated from retinas after using TriZol (Invitrogen) as per the manufacturer's protocol. Total RNA, at least 500 ng, was reverse transcribed using an ABI High Capacity cDNA Reverse Transcription Kit according to the manufacturer's protocol. For quantitation of mRNA, qRT-PCR was performed using Taqman RT-PCR assay. The sequence of the Taqman (R) Gene Expression Assay primers used herein are presented in supplementary Table 2, available in an online appendix.

For cell culture studies, qRT-PCR was performed using QuantiTech SYBR Green PCR Kit (Qiagen) and the following QuantiTech Primer Assay kits (Qiagen) following the manufacturer's protocol: β-actin (Rn_Actb_1_SG QuantiTect Primer Assay NM_031144), VEGFA (Rn_RGD:619991_1_SG QuantiTect Primer Assay NM_001110335), and 4E-BP1 (Rn_Eif4ebp1_1_SG QuantiTect Primer Assay NM_053857).

Statistical analysis. Results from the retina of diabetic animals were compared by ANOVA or Student t test to those from the retina of their nondiabetic counterparts using Prism 4 (GraphPad Software, Inc.). Where appropriate, data were log-transformed for normality. Data from untreated control cells were compared either by ANOVA or Student t test, whichever appropriate, with that from their treated counterparts using Prism 4. The data are presented as mean ± SEM; $P < 0.05$ was considered statistically significant.

RESULTS

Type 1 diabetes results in increased VEGF protein, but not mRNA, expression in the retina. Alterations in VEGF expression were assessed by Western blot analysis

of retinal homogenates prepared from control and STZ-induced type 1 diabetic rats at various times after drug administration. Whereas VEGF expression was increased significantly in the retina of diabetic compared with control rats at 2, 4, and 6 weeks (Fig. 1*A*), the relative abundance of VEGF mRNA remained constant (Fig. 1*B*). In addition to constant expression of VEGF mRNA, expression of the transcription factor, HIF-1α, did not differ among the groups (Fig. 1*C*), suggesting that the mechanism for increased VEGF expression was posttranscriptional.

Phosphorylation of eIF2α, eIF4G, and eIF4E is the same in the retina of diabetic compared with control rats. Because the expression of the VEGF mRNA did not change over the time course used above, mechanisms involved in the regulation of mRNA translation were explored that might explain increased expression of the protein. Such mechanisms include changes in phosphorylation of eIF4E, eIF4G, and the α-subunit of eIF2. Therefore, the phosphorylation state of each of these proteins was assessed at various times after STZ treatment. No significant difference in phosphorylation of eIF2α on Ser51 (Fig. 2*A*), eIF4G on Ser1108 (Fig. 2*B*), or eIF4E on Ser209 (Fig. 2*C*) was observed in the retina of diabetic compared with control rats at 1, 2, 4, or 6 weeks of diabetes.

Increased association of 4E-BP1 with eIF4E is a result of increased expression of 4E-BP1 in the retina of diabetic rats. Another mechanism through which the selection of mRNAs for translation is regulated involves the sequestration of eIF4E by 4E-BP1 (30). Therefore, 4E-BP1 association with eIF4E was assessed, and, as shown in Fig. 3*A*, a significant increase in 4E-BP1 associated with eIF4E was detected in the retina of diabetic compared with control rats, with no change in the amount of 4E-BP2 bound to eIF4E (Fig. 3*A*). The increased association was attributed to both a reduction in the relative phosphorylation of 4E-BP1 on T37/46, a key regulatory phosphorylation site (Fig. 3*B*), and to increased expression of 4E-BP1 (Fig. 3*C*). The time course of changes in 4E-BP1 expression paralleled that observed for VEGF (Fig. 1*A*). 4E-BP1 mRNA expression was unchanged (Fig. 3*D*).

VEGF and 4E-BP1 expression are coordinated in a genetic model of type 1 diabetes. The $Ins2^{Akita}$ mutation is a single amino acid substitution (C96Y) in the *insulin 2* gene that disrupts disulfide bond formation between the A and B chains, resulting in misfolding of proinsulin. The accumulation of misfolded protein leads to ER stress and, ultimately, β-cell apoptosis and development of hypoinsulinemia and hyperglycemia (22). These mice have been used in recent studies to investigate diabetic complications in light of the similar disease progression and characteristics to that of the established STZ-induced model of type 1 diabetes, including increased retinal vascular permeability and elevated apoptosis (22). Thus, to further evaluate the correlation between increased VEGF and 4E-BP1 expression observed in the STZ-induced model of type 1 diabetes in the rat, retinas were harvested from $Ins2^{Akita}$ mice at various time points and analyzed for VEGF and 4E-BP1 protein and mRNA expression. The time course for increased VEGF expression in the $Ins2^{Akita}$ mice was delayed compared with that of the STZ-induced diabetic rat, but the elevated expression of VEGF and 4E-BP1 protein (Fig. 4*A* and B, respectively) were similar in both models of diabetes.

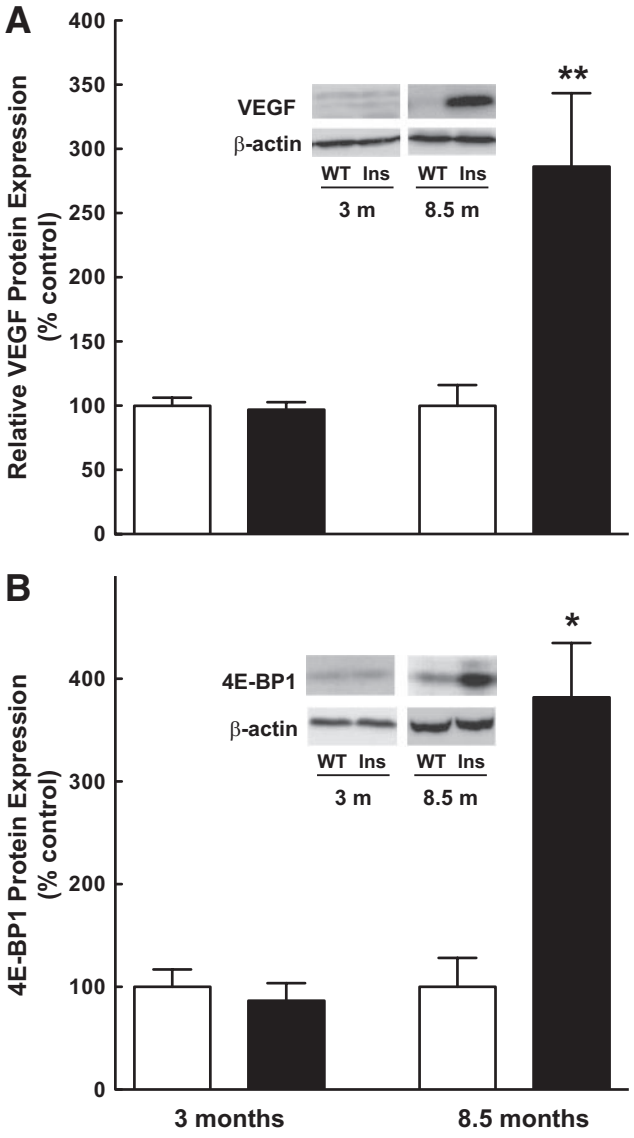

FIG. 4. VEGF expression increases concomitantly with 4E-BP1 expression in $Ins2^{Akita}$ diabetic mice. *A*: Western blot analysis of VEGF expression. Sixty μg of protein was loaded per lane. Values represent the mean expressed as a percentage of control samples ± SEM. Data are representative of retinas from seven wild-type (WT) and four $Ins2^{Akita}$ diabetic (Ins) mice at 3 months, and three WT and three $Ins2^{Akita}$ diabetic mice at 8.5 months of age; control (white bars) and diabetic (black bars) animals. *B*: Western blot analysis of 4E-BP1 expression in Lambda phosphatase-treated retinal extracts. Sixty μg of protein was loaded per lane. *P < 0.01, **P < 0.001 versus corresponding control value.

Ablation of 4E-BP1 prevents the diabetes-induced increase in VEGF expression. If an increase in 4E-BP1 availability is necessary for the increased expression of VEGF, then the absence of 4E-BP1 would be expected to prevent the diabetes-induced change in VEGF expression. To test this hypothesis, retinas from control and STZ-induced diabetic, wild-type, and 4E-BP1 and 4E-BP2 double knockout (*Eif4ebp1*;*Eif4ebp2*) mice were analyzed. While retinal 4E-BP1 protein was detected in *Eif4ebp1*;*Eif4ebp2* wild-type mice, the protein was undetectable in the retinal extracts from *Eif4ebp1*;*Eif4ebp2* double knockout mice, confirming lack of 4E-BP1 expression in these mice (Fig. 5*A*). After 5 weeks of STZ-induced diabetes, VEGF expression was significantly higher in the retina of the diabetic compared with the control *Eif4ebp1*;*Eif4ebp2*

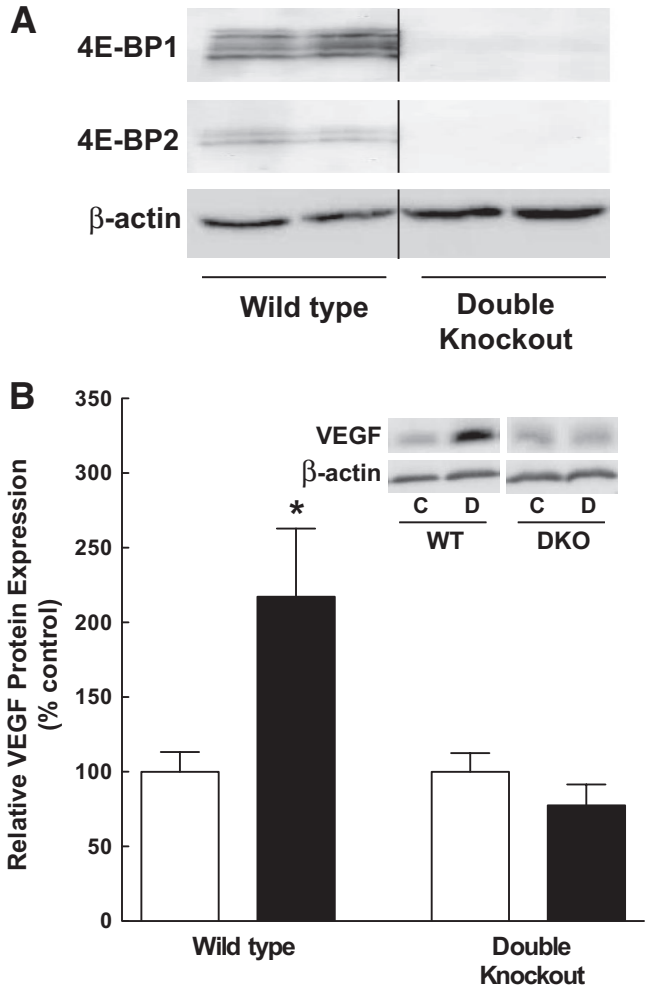

FIG. 5. Ablation of 4E-BP1/2 in mice attenuates the diabetes-induced increase in VEGF expression. *A*: Western blot analysis of 4E-BP1/2 protein expression in the retina of wild-type (WT) and *Eif4ebp1*;*Eif4ebp2* double knockout (DKO) control mice. Four-week-old mice were injected with STZ as described in RESEARCH DESIGN AND METHODS, and 5 weeks later protein (60 μg) was analyzed from six WT and six DKO mice. Representative blots are shown. All samples were run on the same gel, but not in contiguous lanes. *B*: Western blot analysis of VEGF expression in the retina of WT and DKO control and diabetic mice. Protein (60 μg) was analyzed from 12 control and 12 diabetic wild-type mice, and 7 control and 8 diabetic DKO mice; control (white bars) and diabetic (black bars) animals. Values represent the mean ± SEM. **P* < 0.05 versus corresponding control value.

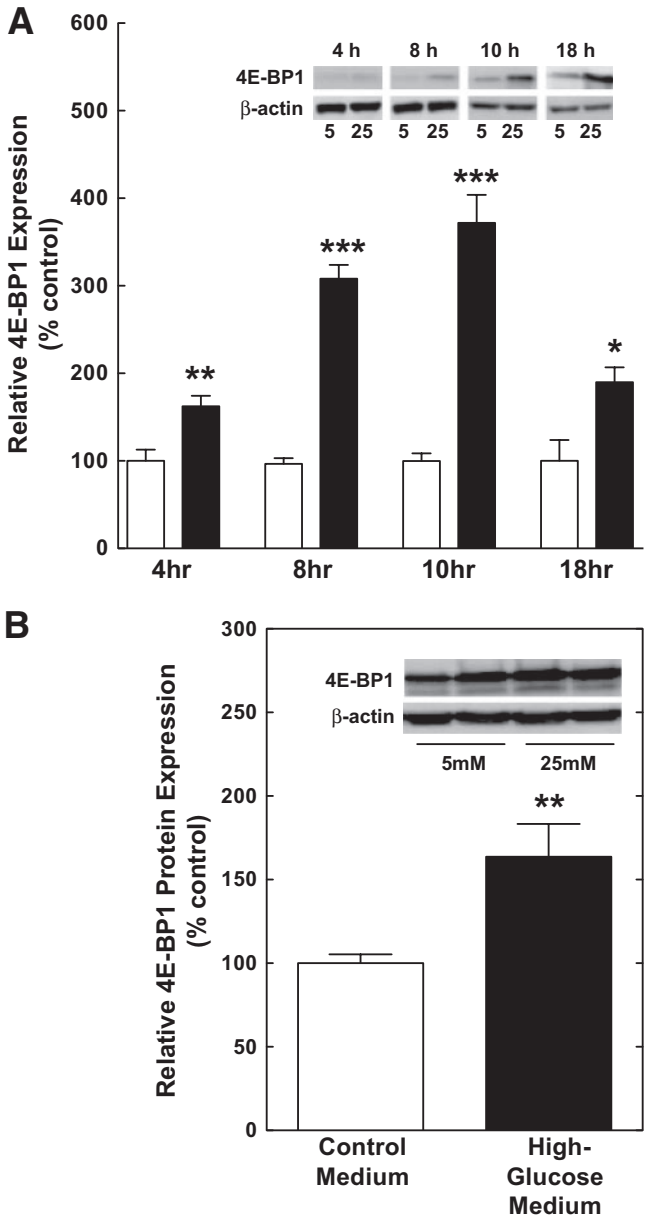

FIG. 6. 4E-BP1 expression is increased under hyperglycemic conditions. *A*: TR-MUL cells were exposed to either control medium (white bars) or high-glucose medium (black bars), and cells were harvested at the indicated time points. Lysates containing 30 μg of protein were subjected to Lambda phosphatase treatment and then subjected to Western blot analysis for 4E-BP1 protein quantitation. Values represent the mean expressed as a percentage of the control ± SEM of 8 or 6 dishes of cells incubated in control or high-glucose medium for 4 h, respectively, 8 or 6 dishes of cells incubated in control or high-glucose medium for 8 h, respectively, 21 or 19 dishes of cells incubated in control or high-glucose medium for 10 h, respectively, 6 or 6 dishes of cells incubated in control or high-glucose medium for 18 h, respectively. *B*: MIO-M1 cells were incubated in control or high-glucose medium, and cells were harvested 10 h later. Cell lysates containing 30 μg of protein were subjected to Lambda phosphatase treatment and then analyzed by Western blot analysis for 4E-BP1. Values represent the mean expressed as a percentage of the control ± SEM of 8 and 6 dishes of cells incubated in control or high-glucose medium, respectively. **P* < 0.05, ***P* < 0.01, ****P* < 0.001 versus corresponding control value.

wild-type mice. In contrast, diabetes had no effect on VEGF expression in the retina of *Eif4ebp1*;*Eif4ebp2* double knockout mice (Fig. 5*B*), despite severe hyperglycemia (supplementary Fig. 1*C*). This result demonstrates that an increase in 4E-BP1 availability is necessary for the diabetes-induced increase in VEGF expression.

Hyperglycemic conditions induce 4E-BP1 expression and association with eIF4E in retinal Müller cells in culture. To assess whether hyperglycemic conditions contribute to the increase in 4E-BP1 and VEGF expression in the retina of diabetic animals, TR-MUL Müller cells were incubated in either control or high-glucose medium for various times. 4E-BP1 expression was significantly increased 4 h after exposure to high glucose and continued to be elevated through 18 h of treatment (Fig. 6*A*). As the maximal increase in 4E-BP1 occurred at ~10 h of treatment, this time point was selected for further studies. An increase in 4E-BP1 expression was also observed in the human Müller cell line, MIO-M1 (Fig. 6*B*), in response to incubation in high-glucose medium, demonstrating that the effect of hyperglycemic conditions was not specific for TR-MUL cells. Although 4E-BP1 protein content was significantly increased at all time points, the expression of

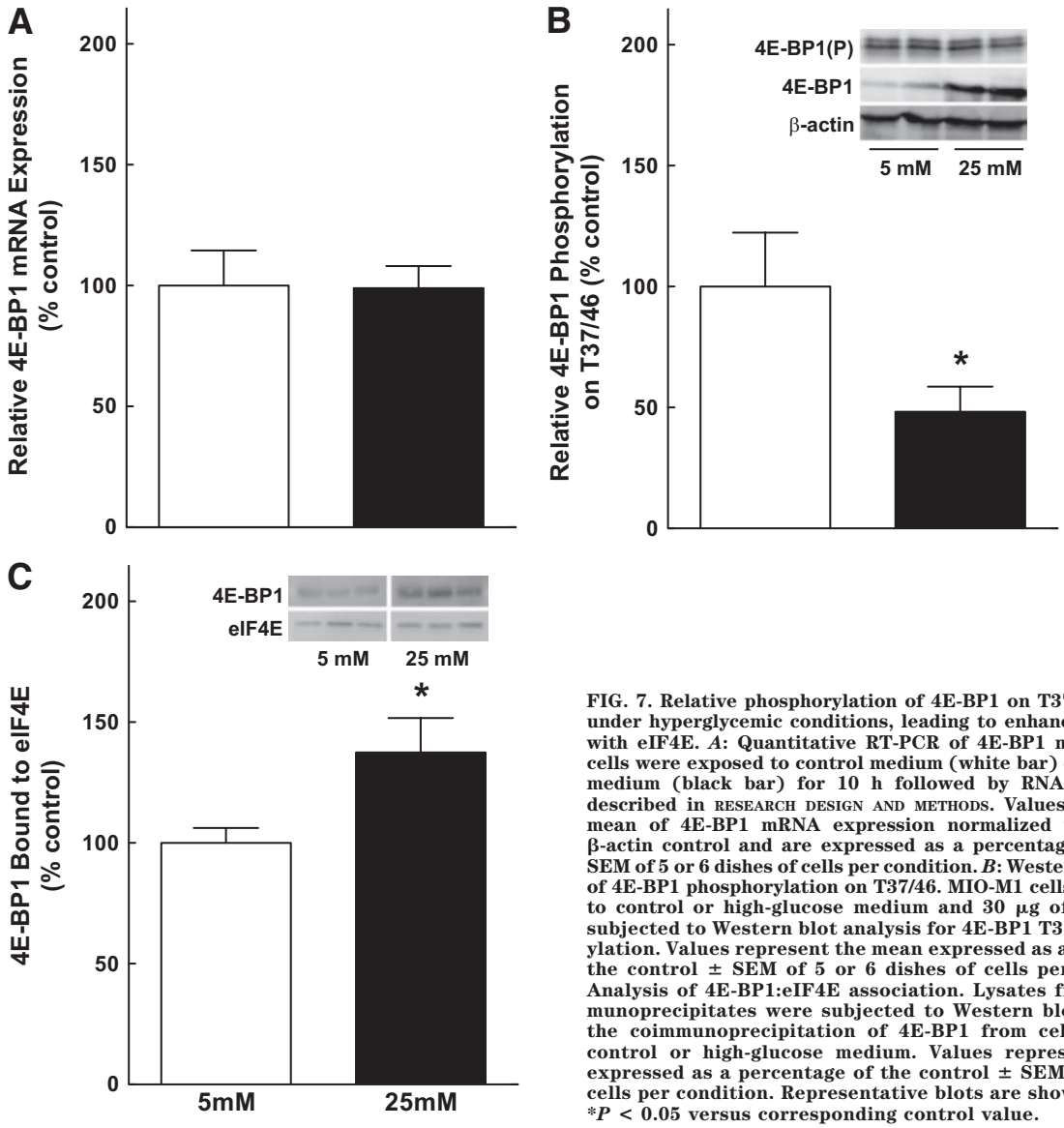

FIG. 7. Relative phosphorylation of 4E-BP1 on T37/46 is reduced under hyperglycemic conditions, leading to enhanced association with eIF4E. *A*: Quantitative RT-PCR of 4E-BP1 mRNA. TR-MUL cells were exposed to control medium (white bar) or high-glucose medium (black bar) for 10 h followed by RNA extraction as described in RESEARCH DESIGN AND METHODS. Values represent the mean of 4E-BP1 mRNA expression normalized to an internal β-actin control and are expressed as a percentage of control ± SEM of 5 or 6 dishes of cells per condition. *B*: Western blot analysis of 4E-BP1 phosphorylation on T37/46. MIO-M1 cells were exposed to control or high-glucose medium and 30 μg of protein were subjected to Western blot analysis for 4E-BP1 T37/46 phosphorylation. Values represent the mean expressed as a percentage of the control ± SEM of 5 or 6 dishes of cells per condition. *C*: Analysis of 4E-BP1:eIF4E association. Lysates from eIF4E immunoprecipitates were subjected to Western blot analysis for the coimmunoprecipitation of 4E-BP1 from cells exposed to control or high-glucose medium. Values represent the mean expressed as a percentage of the control ± SEM of 6 dishes of cells per condition. Representative blots are shown as an inset. *$P < 0.05$ versus corresponding control value.

4E-BP1 mRNA was similar among groups (Fig. 7*A*). Additionally, hyperglycemic conditions caused a decrease in the relative phosphorylation of 4E-BP1 on T37/46 (Fig. 7*B*). Increased expression and decreased phosphorylation resulted in a significant increase in the amount of 4E-BP1 bound to eIF4E, as measured in eIF4E immunoprecipitates (Fig. 7*C*). Thus, similar to the effect observed in the retina of diabetic rodents, 4E-BP1 expression was increased in response to hyperglycemic conditions in Müller cells in culture. The increased VEGF expression in Müller cells is consistent with the immunolocalization of VEGF in human eyes of patients with diabetes (31).

Induction of VEGF secretion under hyperglycemic conditions requires 4E-BP1 expression. To determine whether hyperglycemic conditions resulted in the induction of VEGF, medium was collected for measurement of VEGF secretion by ELISA. After 10 h of high-glucose treatment, the VEGF concentration in the cell culture medium was significantly elevated for VEGFA content (Fig. 8*A*). However, there was no change in the expression of VEGFA mRNA in the cell lysates (Fig. 8*B*), suggesting a posttranscriptional mechanism for the stimulated production of VEGF. VEGF secretion was also stimulated in MIO-M1 cells incubated in the high-glucose medium compared with the control medium (Fig. 8*C*).

To confirm the dependence of VEGF induction on 4E-BP1 expression, wild-type and *Eif4ebp1*;*Eif4ebp2* double knockout MEFs were exposed to either control or high-glucose medium for 10 h. Expression of 4E-BP1 and 4E-BP2 was undetectable in the double knockout cells (data not shown). As observed in Müller cells, 4E-BP1 expression was increased in wild-type MEFs during hyperglycemic conditions (data not shown), and this was associated with a 2.5-fold stimulation of VEGF secretion into the medium (Fig. 8*D*). Secretion of VEGF from double knockout MEFs, on the other hand, was not stimulated under hyperglycemic conditions, confirming the requirement for increased 4E-BP1 expression (Fig. 8*D*).

DISCUSSION

In the present study, VEGF expression was increased, without a change in VEGF mRNA expression, in the retina of three animal models of type 1 diabetes: STZ-induced diabetic rats and mice and $Ins2^{Akita}$ mice. An increase in VEGF expression also occurred in the absence of changes

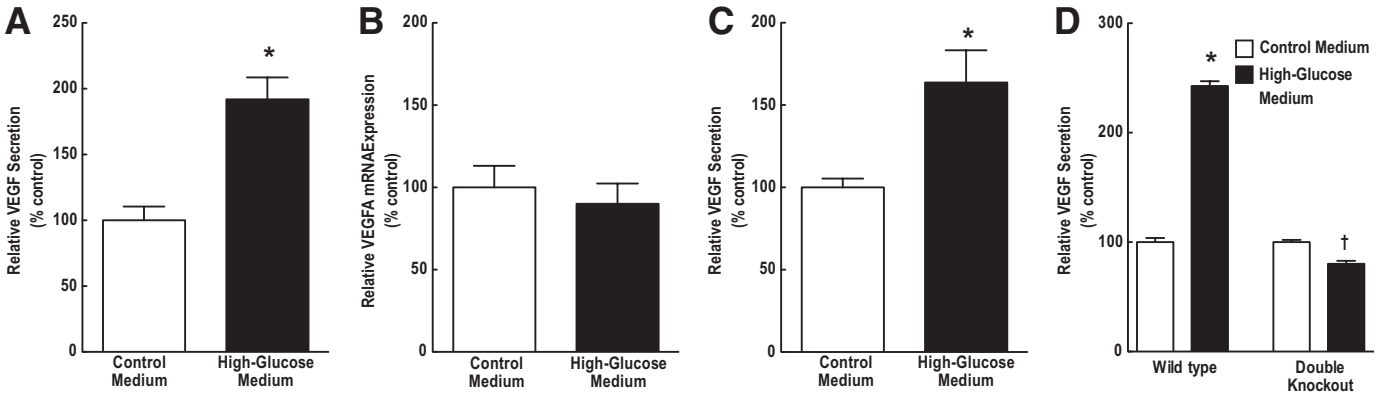

FIG. 8. Hyperglycemic conditions stimulate secretion of VEGF in retinal Müller cells, but not in *Eif4ebp1;Eif4ebp2* double knockout (DKO) MEFs. *A*: Analysis of VEGF secretion. Medium was collected from TR-MUL cells exposed to control medium (white bar) or high-glucose medium (black bar) and subjected to ELISA analysis of VEGFA concentration. VEGF was normalized to protein content in the cell lysates. Values represent the mean expressed as a percentage of the control ± SEM of 6 dishes of cells per condition. *B*: Quantitative RT-PCR of VEGF mRNA. RNA was extracted from TR-MUL cells exposed to control or high-glucose medium followed by RNA isolation as described in RESEARCH DESIGN AND METHODS. Values represent the mean of 4E-BP1 mRNA expression normalized to an internal β-actin mRNA control and are expressed as a percentage of control ± SEM of 6 dishes of cells per condition. *C*: Analysis of VEGF secretion in the human Müller cell line, MIO-M1. Medium was collected from TR-MUL cells exposed to control or high-glucose medium and subjected to ELISA for measurement of VEGFA concentration as described above. Values represent the mean expressed as a percentage of the control ± SEM of 6 dishes of cells per condition. *D*: Analysis of VEGF secretion. Medium was collected from *Eif4ebp1;Eif4ebp2* WT and DKO MEFs exposed to control or high-glucose medium and subjected to ELISA for VEGFA concentration. Values represent the mean expressed as a percentage of the control ± SEM of 9 dishes of cells of WT cells per condition and 6 dishes of double-knockout cells per condition. *$P < 0.001$, †$P < 0.01$ when compared with DKO cells maintained in control medium.

in VEGF mRNA expression in two different Müller cell lines as well as in MEFs exposed to hyperglycemic conditions. These findings suggest that VEGF expression is regulated in a manner that is independent of changes in expression of the message. Although other groups have reported an increase in VEGF mRNA expression in the retina of diabetic animals (32,33), under the conditions used in the present study, no difference was detected.

The results presented herein indicate that 4E-BP1/2 is necessary for the increased expression of VEGF in the retina during diabetes, as the absence of the binding proteins prevents the change. 4E-BP1/2 is also required for the increase in VEGF expression in MEFs maintained in culture under hyperglycemic conditions, as VEGF expression did not increase in 4E-BP1/2 double knockout MEFs exposed to hyperglycemic conditions. In both the retina and in cells in culture, the increase in 4E-BP1 expression led to enhanced binding to eIF4E. Under conditions promoting eIF4E sequestration into the eIF4E·4E-BP1 complex, there is a switch to cap-independent translation, making mRNAs that are normally inefficiently translated, such as the one encoding VEGF, more competitive for translation (33–37). While further studies are required to identify the exact mechanism of 4E-BP1/2-induced regulation of VEGF mRNA translation, it is likely that increased VEGF internal ribosome entry sites utilization accounts for the enhanced expression of the protein.

Increased 4E-BP1 protein content in the absence of changes in 4E-BP1 mRNA expression suggests regulation at the posttranscriptional level in both the retina of diabetic animals and in cells in culture exposed to hyperglycemic conditions. However, unlike the VEGF mRNA, the mRNAs encoding mouse and human 4E-BP1 have relatively short 5′-UTRs that lack significant secondary structure in prediction models. Moreover, the 5′-UTR of the 4E-BP1 mRNA lacks other regulatory sequences that might be involved in translational regulation, such as open reading frames or terminal oligopyrimidine tracts. Although other translational regulatory mechanisms such as microRNAs cannot be discounted, changes in the rate of degradation may contribute to alterations in 4E-BP1 expression. In this regard, evidence for proteasome-dependent degradation of 4E-BP1 has been shown by accumulation of the protein after proteasome inhibition (34) and by ubiquitin immunoprecipitation (35). In the present study, increased binding of 4E-BP1 to eIF4E in the retina of diabetic rats is consistent with possible decreased ubiquitination of 4E-BP1, because previous studies (35) have shown inefficient binding of ubiquitinated 4E-BP1 to eIF4E. Whether or not 4E-BP1 degradation is decreased in the retina of diabetic rodents will be explored in future studies.

A role for 4E-BP1 in regulating VEGF mRNA translation has also been reported in immortalized proximal tubular epithelial (MCT) cells (36). Treatment of MCT cells with angiotensin II promotes increased phosphorylation of 4E-BP1 and recruitment of VEGF mRNA into polysomes. Moreover, incubation in medium containing 30 mmol/l instead of 5 mmol/l glucose leads to increased synthesis of angiotensinogen, a precursor of angiotensin II, as well as VEGF (37). Together these data suggest that elevations in glucose concentration may promote VEGF mRNA translation by increasing expression of angiotensin II, and subsequently 4E-BP1 phosphorylation. Angiotensin II has also been implicated in changes in VEGF expression in the retina of diabetic rodents (38–40). However, in the animal models of diabetes used in those studies, VEGF mRNA expression was increased, a finding not observed in the present study. Further, in the present study, the 4E-BP1 content increased causing a relative decrease in the amount of phosphorylated 4E-BP1, suggesting a distinct mechanism from that observed in MCT cells. Whether or not changes in angiotensin II expression might be involved in the increase in VEGF expression observed in the models of diabetes used herein is unknown.

In the present study, VEGF expression was increased in the retina of diabetic compared with control rats as early as 2 weeks of STZ-induced type 1 diabetes. The elevated expression was sustained for at least 6 weeks but returned to basal levels by 12 weeks. Many studies have docu-

mented that the vascular pathology associated with diabetic retinopathy, such as vascular permeability (41), appearance of acellular capillaries (42), and endothelial apoptosis (43), occur after prolonged periods, for example, 3–8 months, of diabetes in rodents, while other studies have observed vascular changes by 1 week (44). One study (33) reported blood–retinal barrier breakdown in response to a near twofold increase in VEGF expression after only 8 days of diabetes. The increase in permeability was entirely prevented by treatment with a chimeric VEGF receptor (33). Therefore, increased VEGF expression has been observed in multiple animal models, but the time of increase varies with the model and method of diabetes induction as was observed within this study comparing VEGF expression in rat and mouse models of type 1 diabetes.

In the present study, three rodent models of type 1 diabetes yielded similar results in increased expression of VEGF and 4E-BP1. Together, the evidence from these studies strongly suggests that 4E-BP1 is a key modulator of translational control of VEGF expression in the retina during diabetes. Further details about the regulation of VEGF expression may lead to novel therapies to control abnormal vascular permeability and angiogenesis in diabetic retinopathy.

ACKNOWLEDGMENTS

T.W.G. is the Jack and Nancy Turner Professor. This project was funded by a grant from the Juvenile Diabetes Research Foundation International (4-2002-455) and a grant from The Pennsylvania Department of Health using Tobacco Settlement Funds. The Department specifically disclaims responsibility for any analyses, interpretations, or conclusions. No potential conflicts of interest relevant to this article were reported.

T.L.S. researched data and wrote the first draft of the manuscript. D.A.A., N.S., and T.W.G. contributed to discussion and reviewed the manuscript. S.R.K. designed experiments, contributed to discussion, and wrote the manuscript. L.S.J. designed experiments, contributed to discussion, and reviewed/edited the manuscript.

The authors thank The Pennsylvania State College of Medicine JDRF Animal Core for generating the animal models of type 1 diabetes used in the present study. The authors also thank Dr. Patrice E. Fort for his collaborative effort, Dr. Ken-ichi Hosoya (Toyama Medical and Pharmaceutical University) for providing the TR-MUL cells, and Dr. G. Astrid Limb (University College of London) for providing the MIO-M1 cells.

REFERENCES

1. Saaddine JB, Honeycutt AA, Narayan KM, Zhang X, Klein R, Boyle JP. Projection of diabetic retinopathy and other major eye diseases among people with diabetes mellitus: United States, 2005–2050. Arch Ophthalmol 2008;126:1740–1747
2. Adamis AP, Miller JW, Bernal MT, D'Amico DJ, Folkman J, Yeo TK, Yeo KT. Increased vascular endothelial growth factor levels in the vitreous of eyes with proliferative diabetic retinopathy. Am J Ophthalmol 1994;118:445–450
3. Aiello LM, Cavallerano J. Diabetic retinopathy. Curr Ther Endocrinol Metab 1994;5:436–446
4. Aiello LP, Avery RL, Arrigg PG, Keyt BA, Jampel HD, Shah ST, Pasquale LR, Thieme H, Iwamoto MA, Park JE. Vascular endothelial growth factor in ocular fluid of patients with diabetic retinopathy and other retinal disorders. N Engl J Med 1994;331:1480–1487
5. Miller JW, Adamis AP, Shima DT, D'Amore PA, Moulton RS, O'Reilly MS, Folkman J, Dvorak HF, Brown LF, Berse B. Vascular endothelial growth factor/vascular permeability factor is temporally and spatially correlated with ocular angiogenesis in a primate model. Am J Pathol 1994;145:574–584
6. Pierce EA, Avery RL, Foley ED, Aiello LP, Smith LE. Vascular endothelial growth factor/vascular permeability factor expression in a mouse model of retinal neovascularization. Proc Natl Acad Sci U S A 1995;92:905–909
7. Okamoto N, Tobe T, Hackett SF, Ozaki H, Vinores MA, LaRochelle W, Zack DJ, Campochiaro PA. Transgenic mice with increased expression of vascular endothelial growth factor in the retina: a new model of intraretinal and subretinal neovascularization. Am J Pathol 1997;151:281–291
8. Spilsbury K, Garrett KL, Shen WY, Constable IJ, Rakoczy PE. Overexpression of vascular endothelial growth factor (VEGF) in the retinal pigment epithelium leads to the development of choroidal neovascularization. Am J Pathol 2000;157:135–144
9. Kim SH, Roth KA, Moser AR, Gordon JI. Transgenic mouse models that explore the multistep hypothesis of intestinal neoplasia. J Cell Biol 1993;123:877–893
10. Millauer B, Shawver LK, Plate KH, Risau W, Ullrich A. Glioblastoma growth inhibited in vivo by a dominant-negative Flk-1 mutant. Nature 1994;367:576–579
11. Aiello LP, Pierce EA, Foley ED, Takagi H, Chen H, Riddle L, Ferrara N, King GL, Smith LE. Suppression of retinal neovascularization in vivo by inhibition of vascular endothelial growth factor (VEGF) using soluble VEGF-receptor chimeric proteins. Proc Natl Acad Sci U S A 1995;92:10457–10461
12. Klos KS, Wyszomierski SL, Sun M, Tan M, Zhou X, Li P, Yang W, Yin G, Hittelman WN, Yu D. ErbB2 increases vascular endothelial growth factor protein synthesis via activation of mammalian target of rapamycin/p70S6K leading to increased angiogenesis and spontaneous metastasis of human breast cancer cells. Cancer Res 2006;66:2028–2037
13. Levy AP, Levy NS, Wegner S, Goldberg MA. Transcriptional regulation of the rat vascular endothelial growth factor gene by hypoxia. J Biol Chem 1995;270:13333–13340
14. Slomiany MG, Rosenzweig SA. Hypoxia-inducible factor-1-dependent and -independent regulation of insulin-like growth factor-1-stimulated vascular endothelial growth factor secretion. J Pharmacol Exp Ther 2006;318:666–675
15. Kapp LD, Lorsch JR. The molecular mechanics of eukaryotic translation. Annu Rev Biochem 2004;73:657–704
16. Huez I, Créancier L, Audigier S, Gensac MC, Prats AC, Prats H. Two independent internal ribosome entry sites are involved in translation initiation of vascular endothelial growth factor mRNA. Mol Cell Biol 1998;18:6178–6190
17. Bornes S, Boulard M, Hieblot C, Zanibellato C, Iacovoni JS, Prats H, Touriol C. Control of the vascular endothelial growth factor internal ribosome entry site (IRES) activity and translation initiation by alternatively spliced coding sequences. J Biol Chem 2004;279:18717–18726
18. Pause A, Belsham GJ, Gingras AC, Donzé O, Lin TA, Lawrence JC Jr, Sonenberg N. Insulin-dependent stimulation of protein synthesis by phosphorylation of a regulator of 5′-cap function. Nature 1994;371:762–767
19. Haghighat A, Mader S, Pause A, Sonenberg N. Repression of cap-dependent translation by 4E-binding protein 1: competition with p220 for binding to eukaryotic initiation factor-4E. Embo J 1995;14:5701–5709
20. Mader S, Lee H, Pause A, Sonenberg N. The translation initiation factor eIF-4E binds to a common motif shared by the translation factor eIF-4 gamma and the translational repressors 4E-binding proteins. Mol Cell Biol 1995;15:4990–4997
21. Brucklacher RM, Patel KM, VanGuilder HD, Bixler GV, Barber AJ, Antonetti DA, Lin CM, LaNoue KF, Gardner TW, Bronson SK, Freeman WM. Whole genome assessment of the retinal response to diabetes reveals a progressive neurovascular inflammatory response. BMC Med Genomics 2008;1:26
22. Barber AJ, Antonetti DA, Kern TS, Reiter CE, Soans RS, Krady JK, Levison SW, Gardner TW, Bronson SK. The Ins2Akita mouse as a model of early retinal complications in diabetes. Invest Ophthalmol Vis Sci 2005;46:2210–2218
23. Le Bacquer O, Petroulakis E, Paglialunga S, Poulin F, Richard D, Cianflone K, Sonenberg N. Elevated sensitivity to diet-induced obesity and insulin resistance in mice lacking 4E-BP1 and 4E-BP2. J Clin Invest 2007;117:387–396
24. Rannels SR, Rannels DE, Pegg AE, Jefferson LS. Glucocorticoid effects on peptide-chain initiation in skeletal muscle and heart. Am J Physiol 1978;235:E134–E139
25. Harhaj NS, Felinski EA, Wolpert EB, Sundstrom JM, Gardner TW, Antonetti DA. VEGF activation of protein kinase C stimulates occludin phosphorylation and contributes to endothelial permeability. Invest Ophthalmol Vis Sci 2006;47:5106–5115

26. Sun H, Lu CH, Shi H, Gao L, Yao SQ. Peptide microarrays for high-throughput studies of Ser/Thr phosphatases. Nat Protoc 2008;3:1485–1493
27. Kimball SR, Horetsky RL, Jefferson LS. Implication of eIF2B rather than eIF4E in the regulation of global protein synthesis by amino acids in L6 myoblasts. J Biol Chem 1998;273:30945–30953
28. Kimball SR, Jurasinski CV, Lawrence JC, Jr, Jefferson LS. Insulin stimulates protein synthesis in skeletal muscle by enhancing the association of eIF-4E and eIF-4G. Am J Physiol 1997;272:C754–759
29. Shah OJ, Kimball SR, Jefferson LS. Acute attenuation of translation initiation and protein synthesis by glucocorticoids in skeletal muscle. Am J Physiol Endocrinol Metab 2000;278:E76–E82
30. Gingras AC, Kennedy SG, O'Leary MA, Sonenberg N, Hay N. 4E-BP1, a repressor of mRNA translation, is phosphorylated and inactivated by the Akt(PKB) signaling pathway. Genes Dev 1998;12:502–513
31. Amin RH, Frank RN, Kennedy A, Eliott D, Puklin JE, Abrams GW. Vascular endothelial growth factor is present in glial cells of the retina and optic nerve of human subjects with nonproliferative diabetic retinopathy. Invest Ophthalmol Vis Sci 1997;38:36–47
32. Gilbert RE, Vranes D, Berka JL, Kelly DJ, Cox A, Wu LL, Stacker SA, Cooper ME. Vascular endothelial growth factor and its receptors in control and diabetic rat eyes. Lab Invest 1998;78:1017–1027
33. Qaum T, Xu Q, Joussen AM, Clemens MW, Qin W, Miyamoto K, Hassessian H, Wiegand SJ, Rudge J, Yancopoulos GD, Adamis AP. VEGF-initiated blood-retinal barrier breakdown in early diabetes. Invest Ophthalmol Vis Sci 2001;42:2408–2413
34. Walsh D, Mohr I. Phosphorylation of eIF4E by Mnk-1 enhances HSV-1 translation and replication in quiescent cells. Genes Dev 2004;18:660–672
35. Constantinou C, Clemens MJ. Regulation of translation factors eIF4GI and 4E-BP1 during recovery of protein synthesis from inhibition by p53. Cell Death Differ 2007;14:576–585
36. Feliers D, Duraisamy S, Barnes JL, Ghosh-Choudhury G, Kasinath BS. Translational regulation of vascular endothelial growth factor expression in renal epithelial cells by angiotensin II. Am J Physiol Renal Physiol 2005;288:F521–F529
37. Feliers D, Kasinath BS. Mechanism of VEGF expression by high glucose in proximal tubule epithelial cells. Mol Cell Endocrinol 2010;314:136–142
38. Gilbert RE, Kelly DJ, Cox AJ, Wilkinson-Berka JL, Rumble JR, Osicka T, Panagiotopoulos S, Lee V, Hendrich EC, Jerums G, Cooper ME. Angiotensin converting enzyme inhibition reduces retinal overexpression of vascular endothelial growth factor and hyperpermeability in experimental diabetes. Diabetologia 2000;43:1360–1367
39. Nagai N, Izumi-Nagai K, Oike Y, Koto T, Satofuka S, Ozawa Y, Yamashiro K, Inoue M, Tsubota K, Umezawa K, Ishida S. Suppression of diabetes-induced retinal inflammation by blocking the angiotensin II type 1 receptor or its downstream nuclear factor-kappaB pathway. Invest Ophthalmol Vis Sci 2007;48:4342–4350
40. Zhang X, Lassila M, Cooper ME, Cao Z. Retinal expression of vascular endothelial growth factor is mediated by angiotensin type 1 and type 2 receptors. Hypertension 2004;43:276–281
41. Antonetti DA, Lieth E, Barber AJ, Gardner TW. Molecular mechanisms of vascular permeability in diabetic retinopathy. Semin Ophthalmol 1999;14:240–248
42. Hammes HP, Lin J, Bretzel RG, Brownlee M, Breier G. Upregulation of the vascular endothelial growth factor/vascular endothelial growth factor receptor system in experimental background diabetic retinopathy of the rat. Diabetes 1998;47:401–406
43. Mizutani M, Kern TS, Lorenzi M. Accelerated death of retinal microvascular cells in human and experimental diabetic retinopathy. J Clin Invest 1996;97:2883–2890
44. Antonetti DA, VanGuilder HD, Mao-Lin C. Vascular permeability in diabetic retinopathy. In *Diabetic Retinopathy*. Duh EJ, Ed. Clifton, NJ, Humana Press, 2009, p. 333–352